Sirte University Scientific Journal (Applied Sciences) Vol.12(1), June 2022

Photosynthetic of Water Oxidation for $RuPtI_2$ Complexes

Hamid M. Ahmed[1], Mohammed Al-Saker[2] and Sven Rau[3]*
E-mail: *hamid.younis@su.edu.ly*

[1]*Department of Chemistry, Faculty of Sciences, Sirte University, SU, Sirte-Libya.*
[2]*Technical Management, Sirte Oil and Gas Production and Manufacturing Company,Brega–Libya*
[3]*Institute of Inorganic ChemistryI, Ulm University, Albert-Einstein-Allee, Ulm-Germany.*

Abstract

This work elaborates the effect of dynamic irradiation and enhanced mass transport on light-driven molecular water oxidation for RuPtI2 complexes to counteract catalyst deactivation. It highlights the importance of overall reaction design to overcome limiting factors in artificial photosynthesis reactions. Systematic investigation of a homogenous three components ruthenium-based water oxidation system revealed significant potential to enhance the overall catalytic efficiency by synchronizing the timescales of photoreaction and mass transport in a capillary flow reactor. The overall activity could be improved by a factor of more than 20 with respect to the turnover number and a factor of 30 referring to the external energy efficiency by applying low irradiation intensities and high flow rates following them by HPLC.

Keywords: *Water, Oxidation, Ruthenium Catalysts, Irradiation, LED, HPLC.*

1. Introduction

Many heterogeneous and homogenous systems for the photochemical splitting of water have been developed and chemically optimized in regards to molecular components, buffer conditions and pH-ranges [1]. Artificial photosynthetic reactions are so far usually broken down into two half reactions, which are studied separately. Oxidation of water to form oxygen, protons and electrons and reduction of protons to yield hydrogen [2]. The overall performance of photocatalytic reactions depends on a complex interplay between molecular properties of the involved chemical

species, the environment around the active components and the presence of light of suitable intensity and wavelength. The highly ordered and synchronized mechanisms of biological photosynthesis can serve as a source of inspiration: to unleash the full potential of artificial photosynthetic catalysis, a thorough understanding of the interaction between the catalytic species, the micro- and macroscopic mass transport as well as the radiation field is necessary [3]. Thus, catalyst development and reaction engineering need to be combine synergistically [4]. To understand the impact of mass transport and irradiation conditions on the photocatalytic water oxidation, we adopted the well-known system consisting of [(tbbpy)2Ru(tpphz) PtI2](PF6), which acts as single-site water oxidation catalyst (WOC), the photosensitizer [Ru(bpy)2(phen)](PF6)2 PS, bpy = 2,2'-bipyridine (Figure 1) [5,6].

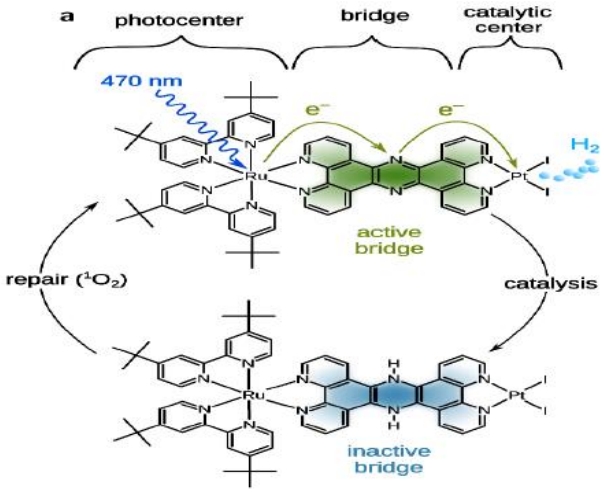

Figure 1. Visible light-driven hydrogen production with a photochemical molecular device (PMD)[6].

Molecular Catalysts for Water Oxidation:

Like their heterogeneous analogues, perhaps the best- characterized homogeneous catalysts rely on the three elements mentioned above as privileged catalysts for water oxidation: manganese, ruthenium, and iridium [7]. The first homogeneous catalyst for water oxidation, Meyer's so-called "Blue Dimer", relies on ruthenium [8]. The use of ruthenium in the first case is likely a consequence of the relative abundance of synthetically accessible complexes. Relatively slower ligand exchange rates also make observation of intermediates more likely. In the case of iridium, it was known to be is

the most active and stable oxide catalyst for water oxidation for many years, but waited for work in the direction of homogeneous catalysis until late in the decade 2000−2010. There is also considerable interest in the use of cheap and base metals as catalysts, which recently been reviewed [9].

Ruthenium Catalysts:

The first homogeneous water-oxidation catalyst, the ruthenium polypyridyl complex reported by Meyer and co-workers in 1982 [10], has emphasized the role of proton-coupled electron-transfer (PCET) processes for water activation [11], as outlined in a recent review [12]. In such processes, oxidation of the metal center causes a pKa shift of water ligands bound at the metal; the net result is activation of bound water upon metal oxidation, giving hydroxo or oxo complexes upon oxidation of the ruthenium center. Enhancing the donor power of the ligand set in each PCET step, by going from aqua to hydroxo to oxo, makes the next oxidation state advance easier to achieve, thus promoting the multielectron oxidation normally considered necessary for water oxidation.

2. Experimental:

Synthesis:

The complexes $[(tbbpy)_2Ru(tpphz)\ PtI_2](PF_6)_2$ and (tpphz) being tetrapyrido[3,2-a:2´ ,3´ -c:2´´,3´´-h:2´´´,3´´´-j]phenazine 4–6, were prepared according to literature [13].

Photochemical water oxidation catalysis:

All studies were carried out in deaerated solvents under argon atmosphere in a hermetically sealed setup. Reference measurements conducted in order to study the impact of mass transport were performed in screw cap GC-vial (diameter: 12.75 ± 0.25 mm, length: 99.00 ± 0.50 mm) equipped with two sensor spots mounted on the glass wall of the reaction vessel. The catalytic solution contained tpphz, phen, and $Ru(tpphz)PtI_2$ (2.6 µM), PS (0.3 mM) and $Na_2S_2O_8$ (10 mM) in a solvent mixture of 96 v-% of aqueous $H_3BO_3/NaHCO_3$ buffer (pH 6.5, 0.08 M H_3BO_3) and 4 v-% MeCN.

Water Electrolysis:

The process of biological water splitting bears resemblance to water electrolysis, in which an electrical potential deference is used to split water at two electrodes. The two half reactions and the overall reaction at acidic pH values are as follows:

$$\text{Anod} \quad 2H_2O \longrightarrow O + 4H^+ + 4e^-$$
$$\text{Cathode} \quad 2H^+ + 2e^- \longrightarrow H_2$$
$$\text{Overall} \quad 2H_2O \longrightarrow O_2 + 2H_2$$

The hydrogen gas fuel can then be collected, stored, and used later. The overall reaction of water splitting was accomplished as early as 1789 [14,15].

Water Oxidation in Energy Storage:

In this process, the sun is used as the most abundant source of renewable energy. The current would demand for energy is approximately 15 terawatts (15×10^{12} Js^{-1}), and the sun can provide more than 50 terawatts of energy in the form of solar light irradiance [16,17].

Oxygen detection:

Determination of oxygen concentrations was carried out with a FireStingO_2 optical oxygen meter (Pyroscience, Germany), using oxygen sensitive optical sensor spots (OXSP5, with optical isolation, Pyroscience, Germany). The spots were glued to the inner glass wall of the respective vessel (transparent silicone glue, SPGLUE, Pyroscience, Germany). The reservoir vessel with attached light guide for the O_2 detection are shown in Figure 2.

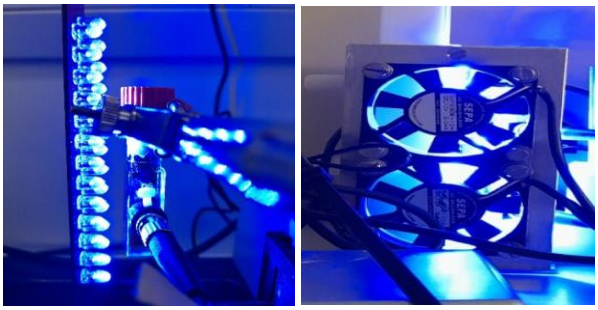

Figure 2. Photography of the used oxygen sensitive optical sensor spots, with 470 nm LED.

Photocatalytic Experiments:

All solutions used were degassed prior to irradiation. In order to produce a stock solution, an exact sample weight was dissolved in 20 mL of acetonitrile. The sample solution of the complexes in the Hight Performance Liquid chromatography (HPLC) vials was then prepared by mixing 1.2 mL of the stock solution, ACN, 0.2 mL of H_2O (10%), and 0.6 mL of TEA under a nitrogen atmosphere. The sample solutions contained 1.17×10^{-4} mol/L photocatalyst. For the experiments, the sample solutions (2 mL) were filled in HPLC vials, which were irradiated for several hours at 470 nm using light-emitting diodes (LEDs, 40−50 mW). The irradiation occurs from below, and the vials are cooled by cooling fans from the side, in order to keep the catalytic solutions at room temperature. After irradiation, the amount of H_2 produced was measured by means of HPLC after 0, 1, 2, 4, %, 10, and 24 h and an average of three samples was taken for calculating the TON and TOF values. H_2 evolution was determined by headspace HPLC using a Bruker Scion gas chromatograph/mass spectrometer, with thermal conductivity detection (column, molecular sieve 5A, 75 m × 0.53 mm i.d.; oven temperature 24 °C; flow rate 2.5 mL/min; detector temperature 200 °C) with argon as the carrier gas.

Irradiation setup of the capillary reactor, a LED Engin LZ1-10B202-000 460 nm LED was used. The LED was purchased soldered on a star PCB and was then screwed onto the heatsink shown in Fig. 3 (including thermal paste). The datasheet states a radiant flux between 1215 mW and 1485 mW or aphoton flux between 4.5 µmol s -1 and 5.5 µmol s -1 for a DC forward current of 1000 mA., A KORAD KA3005P programmable benchtop power supply was used as power supply.

Monitoring Catalytic Conversions with Fiberoptic Oxygen Sensors

A series of measurements using fiber optic oxygen sensors for continuously monitoring the change of oxygen concentration during catalyses at a variety of experimental condition is discussed for elucidating the potential mechanisms of oxygen consumption. The proposed mechanisms for the consumption of the oxygen during the photocatalysis are:

i. Reaction with the reduced catalytic center.
ii. Energy transfer from the excited photocenter to the oxygen.
iii. Electron transfer from the reduced phenanthroline moiety to the oxygen.
iv. Electron transfer from the hydrogenated phenazine moiety to the oxygen.

In order to investigate and potentially verify these proposed mechanisms, different samples were prepared, i.e., catalysts were used after deliberately and selectively eliminating some key ligands from the catalyst and then executing the catalyses while monitoring the consumption.

HPLC Setup:

After washing the column with HPLC Grade acetonitrile/water (50/50 v/v) with a low flow change that suited the mobile phase for appropriately 20-30min until the pressure had stabilised. The injection loop was cleaned by placing the loop in the (load) position and injecting the mobile phase. This was repeated for every change of mobile phase and samples. The absorbance detection wavelength (UV/Vis detector) was 280 nm and depending on experiment and solvents. Figure 3 gives a very nice illustration of the chromatograms of compound $RuPtI_2$, during the irradiation time before and after irradiation.

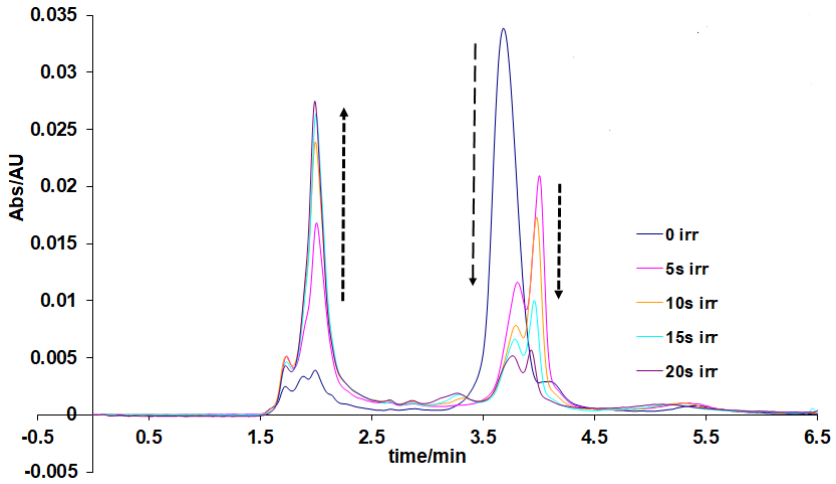

Figure 3 . HPLC traces obtained upon photolysis of $RuPtI_2$Temperature 24^o C. Irradiated in CH_3CN in presence of TEA (15%) and H_2O(10%) using 460 nm LED irradiation from (0-20s) degassing with Ar before irradiation detection wavelength; 460 nm, Mobile Phase CH_3CN:H_2O:CH_3OH with volume ratio 75:15:10 containing 0.10 M KNO_3 Flow rate 2.0 cm^3 min^{-1}.

3. Results and Discussion

The molecular structure of the Ru(tpphz)PtI_2 photocatalyst, consisting of a bis(*tert*-butyl-bipyridine)-ruthenium (II) photocenter, a tetrapyridophenazine (tpphz) bridging ligand and a diiodo-platinum(II) catalytic centre. Photocatalytic hydrogen production with Ru(tpphz)PtI_2 (TON = turnover number). Through the short exposure of the hydrogenated PMD to *in situ* generated singlet oxygen (O_2), the photocatalyst is re-oxidized to its active form and is again applicable for light-driven hydrogen production. By the repetitive active repair of the *damaged* photocatalyst, the long-term activity of the PMD is prolonged to weeks of active hydrogen formation.

The in situ absorption spectra of the catalytic solution show a rapid rise of a new absorption band between 500 nm and 650 nm (Figure 4), which is assigned to reduction of the tpphz bridging unit of the Ru(tpphz)PtI_2 photocatalyst. Besides a fast increase of the absorption intensity, the maximum of the new band slowly shifts hypsochromically from 592 nm to 570 nm with continuous LED irradiation at 455 nm. This is attributed to the formation of the catalytically

inactive species, Ru(tpphzH$_2$)PtI$_2$. No further spectral changes are observed after 48 hours of catalysis. The gray, dashed line shows the UV/vis absorption spectrum of the singly reduced photocatalyst (Ru(tpphz)PtI$_2$) in acetonitrile (-1.35 V *vs.* Fc/Fc$^+$, 0.1 M *n*-Bu$_4$NBF$_4$).

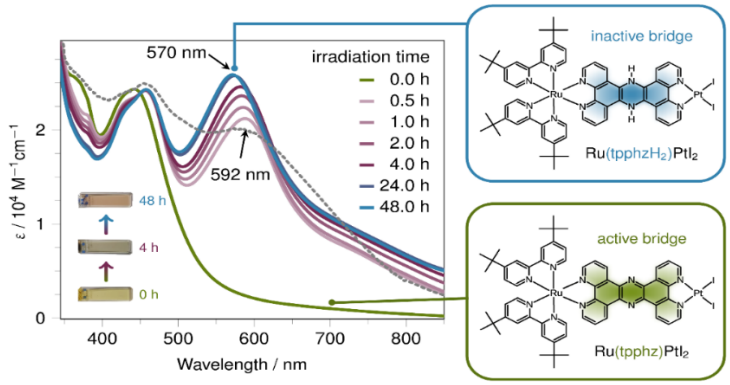

Figure 4. UV/vis absorption spectra of the catalytic solution at different irradiation times.

The spectrum (Figure 5) illustrates the hydrogenated photocatalyst Ru(tpphzH$_2$)PtI$_2$ generated chemically by the reaction of Ru(tpphz)PtI$_2$ with hydrogen. After 1 minute of LED-irradiation (470 nm) under aerobic conditions the *in situ* generated singlet oxygen-driven dehydrogenation of Ru(tpphzH$_2$)PtI$_2$ is almost complete and forms the original (oxidized) form (dark violet line). After 45 min of LED-illumination no significant amounts of the hydrogenated species are detected anymore (bright violet line).

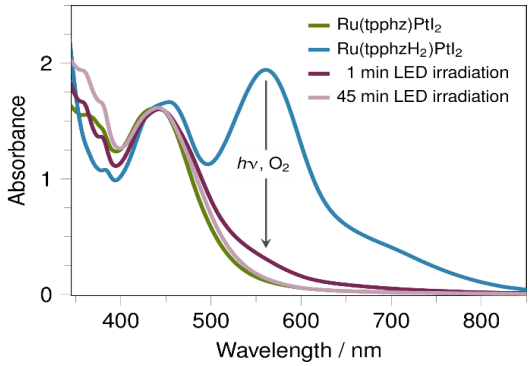

Figure 5. UV/vis absorption spectra showing the dehydrogenation of the photocatalyst Ru(tpphzH$_2$)PtI$_2$ by singlet oxygen.

Reaction of Oxygen with the Reduced Catalytic Center

For potentially verifying this interaction, three different experiments were conducted the same Ruthenium complex, however, using with three different permutations:

(i) $RuPtI_2$,

(ii) $RuPdCl_2$,

(iii) Ru complex without center.

All three experiments yielded largely similar results in terms of oxygen consumption, as showing in Figure 6.

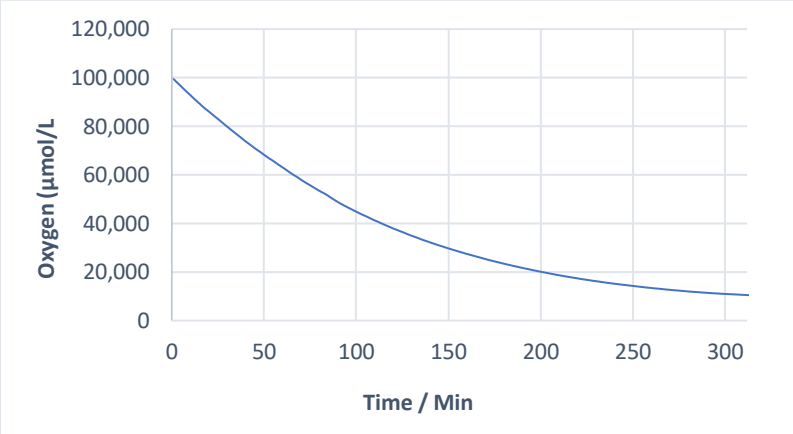

Figure 6. Catalytic center independence of the O_2 consumption

The mechanism proposed herein may procced along two different routes, as shown in Figure 6. As the catalytic center may be excluded as active component responsible for oxygen consumption, the ruthenium photocenter and the tpphz-bridge remain as potential candidates. Regarding the photocenter, two pathways can be considered: (A) either a direct electron transfer to from superoxide or (B) energy transfer by the exited ruthenium center to O_2 forming singlet oxygen [17,18] . Since the latter mechanism would not require the presence of an electron donor (TEA), oxygen consumption of Ru(tpphz) in absence of TEA was investigated.

Route A appears to be the more likely pathway according to these considerations, because of the hydrogenation of the bridging ligand and the further reaction to peroxide, which inherently

consumes oxygen. A similar mechanism was recently published by [19,20]. Route B would be direct electron transfer to oxygen from the excited ruthenium center producing highly reactive superoxide. The actual catalysis process remains similar as already lined out for the first hypothesis i.e., the reaction of oxygen with reduced catalytic center. Demonstrates that the hydrogenation of the bridging ligand still results in the consumption of oxygen (Figure 7).

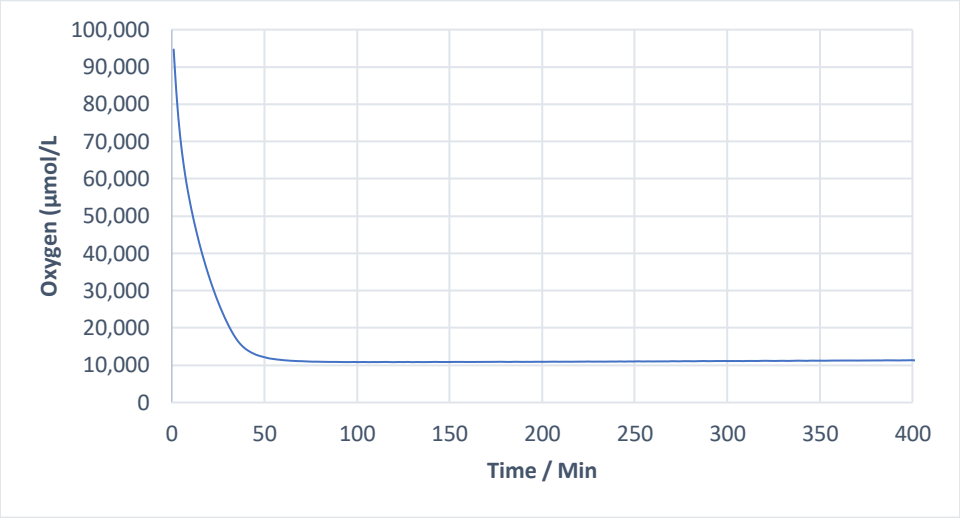

Figure 7. Oxygen consumption behavior using Ru(tpphz) as catalyst.

It is believed that perhaps may imply that the bridging ligand could play a significant role in the oxygen consumption, yet, may not present the sole mechanism for the consumption of the oxygen. The reason for this assumption is that, so far, the trends in the oxygen consumption is no different from the sample with presence of catalytic center [21]. Since the hypothesis from route A (i.e., hydrogenation of the bridging ligand which eventually takes up oxygen to peroxides or superoxides) seemed likely, it was necessary to conduct the experiment without the bridging ligand to how much it contributes to the oxygen consumption.

Electron Transfer from Reduced Phenanthroline Moiety to oxygen

The next experiment was to remove the bridging ligand, and again the cataysis reaction in other to verify the above hypothesis. The aim of this experiment was to determine the contribution of the bridging ligand to the consumption of oxygen. Figure 8 shows the structure of the ruthenium

complex without the bridging ligand and without the catalytic center. However, the electron donor triethylamine (TEA) remained present this series of experiments.

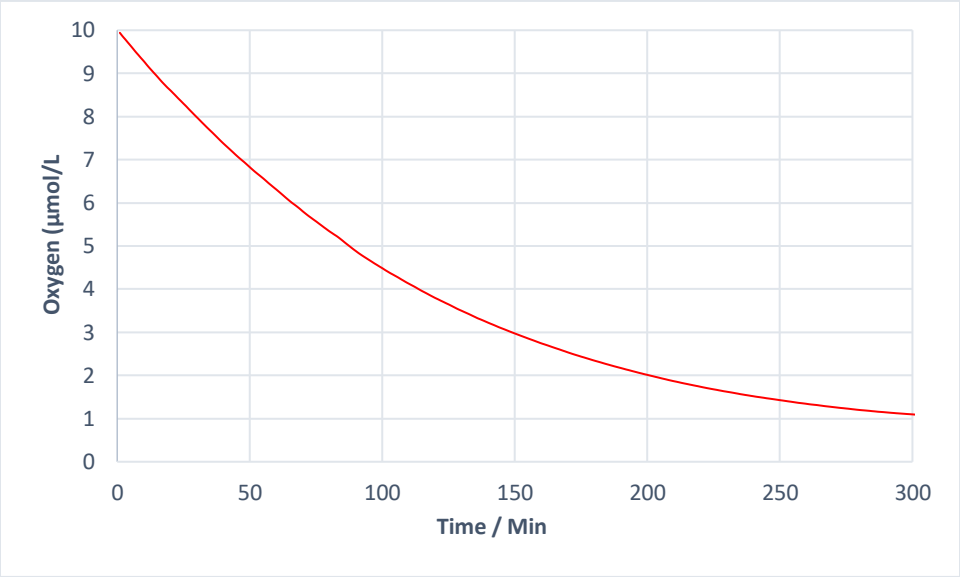

Figure 8. Electron transfer from the reduced phenanthroline moiety to O_2

In the immediately evident that without the bridging ligand the consumption of oxygen is not as rapid as it has been in the previous case with the bridging ligand. The oxygen consumption curve in this case is linear with resulting concentration of the oxygen at approximately 10% after 6 hrs. compared to the catalysis with the bridging ligand, where the oxygen concentration was already down 20 2% in same 6 hrs period, it demonstrates that the bridging ligand is not solely responsible for the consumption of oxygen and certainly not responsible initiating oxygen consumption, but contributes to a significant extent.

From the data shown above, it may be derived that either the ruthenium center or the electron donor (TEA), or the combination of both are responsible for initiating the oxygen consumption during the catalyses. These results directly lead to the next set of experiments.

Catalysis with $RuPtI_2$ Complexes

Oxygen monitoring experiments were also carried out evaluating the catalytic reactions using $RuPtI_2$, which is an alternative stable complex under investigation [22]. Figure 9 illustrates the structures of the complexes under investigation with the only difference being the additional *tert*-butyl groups attached to the improve the stability of the complex. However, they may also limit the transfer of electron from an additional (external) electron donor during catalysis experiments. Hence, the oxygen consumption rates were evaluated in the order to determine the contribution of these functionalities.

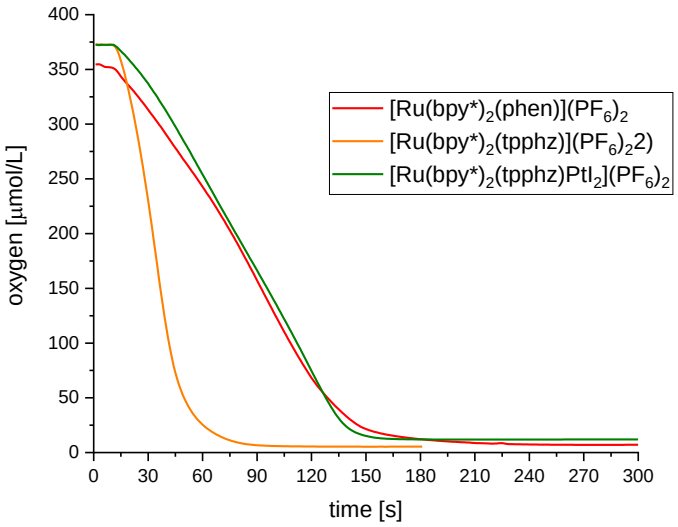

Figure 9. O_2 consumption for $RuPtCl_2$

As expected, both catalysts show the consumption of oxygen. The first sample $[(bpy)_2Rubptz)PtCl_2](PF_6)_2$ revealed a more rapid consumption of oxygen, which expected if the tert-butyl group would indeed hinder the electron transfer rate [23]. This finding is another confirmation that there is always consumption of oxygen during catalysis of such complexes. In a next step, the oxygen consumption behavior was studied during catalysis and following the same process of ligands removal.

4. Conclusions

The primary aim of this work to investigate the utility of luminescence-based fiberoptic oxygen sensors as analytical instrument for quantitively and continuously monitoring the oxygen concentration during chemical reactions, here, to catalytic water splitting. in particular, the catalytic properties, of newly developed hydrogen-producing ruthenium based complex photocatalysts were investigated, which are known to consume oxygen during the catalytic conversion. Using in-situ oxygen probes assists in elucidating the fundamental mechanism of oxygen consumption by facilitating monitoring of the oxygen concentration throughout the entire experimental period. Ruthenium based photocatalyst are usually composed of three main components, namely: (i) the Ru photocenter that serves as light absorbing chromophore, (ii) the $(PF^*_6)_2$ group which serves as a uni-directional electron transfer and bridging ligand, (iii) the Pt-based catalytic center.

In the present study the consumption of oxygen by this complex was determined to result from the action of the electron donor used during the experiments i.e., TEA in combination with the Ru complex and the bridging ligand. The catalytic center was determined not to participate in the oxygen consumption at all. Considering the bridging ligand and the Ru photocenter, it was found that the bridging ligand more significantly contributes to the consumption. More conclusively, without the electron donor present no oxygen consumption is observed in the first place. However, it could also be shown that the presence of oxygen electron is not solely responsible for the consumption of oxygen. Experimental evidence showed that the electron donor may be responsible for initiating the consumption of the oxygen yet, the bridging ligand may be responsible for ongoing oxygen consumption. It is hypothesized that the occurring processes may involve the hydrogenation of the phenazine moiety facilitating the subsequent reaction with oxygen to form hydrogen super oxides.

Conclusively, if the emergence H_2O_2 and other possible by product superoxides can be monitored e.g. electrochemically in solution, then the mechanism of the oxygen consumption can be precisely

nailed down. More importantly, if the hydrogen production can be monitored in situ with electrochemical sensors, it will be a more possibility for the much-desired catalytic water splitting.

References:

1. J. O. Bockris, M. Energy: The Solar-Hydrogen Alternative; Hogbin and Poole: Redfern, Australia, 1975.

2. H. B. Gray, Powering the Planet with Solar Fuel. Nat. Chem. 2009, 1, 7.

3. A. Zouni, Witt, H.-T.; Kern, J.; Fromme, P.; Krauss, N.; Saenger, W.; Orth, P. Crystal Structure of Photosystem II from Synechococcus elongatus at 3.8 Å Resolution. Nature 2001, 409, 739−743.

4. Y. Umena, Kawakami, K.; Shen, J.-R.; Kamiya, N. Crystal Structure of Oxygen-Evolving Photosystem II at a Resolution of 1.9 Å. Nature 2011, 473, 55−60.

5. K. E. hinopoulos, Brudvig, G. W. Cytochrome b559 and Cyclic Electron Transfer within Photosystem II. Biochim. Biophys. Acta, Bioenerg. 2012, 1817, 66−75.

6. (a) J. T. Stock, Orna, M. V., Eds.; In Electrochemistry: American Chemical Soc.: Washington, DC, 1989; (b) Pfeffer, M. G. et al. Active repair of a dinuclear photocatalyst for visible-light-driven hydrogen production. Nat. Chem. 2022, 14(5),500-506.

7. C. W. Cady, Crabtree, R. H.; Brudvig, G. W. Functional Models for the Oxygen-Evolving Complex of Photosystem II. Coord. Chem. Rev. 2008, 252, 444−455.

8. M. G. Pfeffer, T. Kowacs, M. W¨achtler, J. Guthmuller, B. Dietzek, J. G. Vos and S. Rau, Angew. Chem., Int. Ed., 2015, 54(22), 6627–6631.

9. C. Chiorboli, C. A. Bignozzi, F. Scandola, E. Ishow, A. Gourdon and J.-P. Launay, Inorg. Chem., 1999, 38(10), 2402–2410.

10. C. Chiorboli, M. A. J. Rodgers and F. Scandola, J. Am. Chem. Soc., 2003, 125(2), 483–491.

11. (a) Y. Tamaki, K. Koike, T. Morimoto, Y. Yamazaki and O. Ishitani, Inorg. Chem., 2013, 52, 11902–11909; (b) Y. Tamaki, K. Koike, T. Morimoto and O. Ishitani, J. Catal., 2013, 304, 22–28.

12. Y. Miyake, K. Nakajima, K. Sasaki, R. Saito, H. Nakanishi and Y. Nishibayashi, Organometallics, 2009, 28(17), 5240–5243.

13. J. Ferguson, F. Herren, E. R. Krausz, M. Maeder and J. Vrbancich, Coord. Chem. Rev., 1985, 64, 21–39.

14. S. Tschierlei, M. Karnahl, M. Presselt, B. Dietzek, J. Guthmuller, L. Gonz´alez, M. Schmitt, S. Rau and J. Popp, Angew. Chem., Int. Ed., 2010, 49(23), 3981–3984.

15. D. Imanbaew, J. Lang, M. F. Gelin, S. Kaufhold, M. G. Pfeffer, S. Rau and C. Riehn, Angew. Chem., Int. Ed., 2017, 56(20), 5471–5474.

16. M. Martynow, S. Kupfer, S. Rau and J. Guthmuller, Phys. Chem. Chem. Phys., 2019, 21, 9052–9060.

17. B. A. Meyer, T. J. Oxobis(2,2′-bipyridine)- pyridineruthenium(IV) Ion, [(bpy)2(py)RuO]2+. J. Am. Chem. Soc. 1978, 100, 3601−3603.

18. C. J. Gagliardi, Vannucci, A. K.; Concepcion, J. J.; Chen, Z.; Meyer, T. J. The Role of Proton Coupled Electron Transfer in Water Oxidation. Energy Environ. Sci. 2012, 5, 7704−7717.

19. D. Cambie, C. Bottecchia, N. J. W. Straathof, V. Hessel, T. Noe, Chem. Rev. 2016, 116, 10276–10341.

20. R. Matheu, P. Garrido-Barros, M. Gil-Sepulcre, M. Z. Ertem, X. Sala, C. Gimbert-Suriñach, A. Llobet, Nat. Rev. Chem. 2019, 3, 331– 341.

21. J. T. Muckerman, M. Kowalczyk, Y. M. Badiei, D. E. Polyansky, J. J. Concepcion, R. Zong, R. P. Thummel, E. Fujita, Inorg. Chem. 2014, 53, 6904–6913.

22. L. T. Hickey, A. N. Hafeez, H. Robinson, S. A. Jackson, S. C. M. Leal-Bertioli, M. Tester, C. Gao, I. D. Godwin, B. J. Hayes, B. B. H. Wulff, Nat. Biotechnol. 2019, 37, 744–754.

23. M. G. Pfeffer, T. Kowacs, M. Wächtler, J. Guthmuller, B. Dietzek, J. G. Vos, S. Rau, Angew. Chemie - Int. Ed. 2015, 54, 6627–6631.